British Journal of Pharmacology

DOI:10.1111/j.1476-5381.2011.01425.x
www.brjpharmacol.org

RESEARCH PAPER

Characterization of the endocannabinoid system, CB_1 receptor signalling and desensitization in human myometrium

Paul J Brighton[1], Timothy H Marczylo[1], Shashi Rana[1], Justin C Konje[1] and Jonathon M Willets[1,2]

[1]*Endocannabinoid Research Group, Reproductive Sciences Section, Department of Cancer Studies and Molecular Medicine, University of Leicester, Leicester Royal Infirmary, Leicester, UK, and* [2]*Department of Cell Physiology and Pharmacology, Henry Wellcome Building, University of Leicester, Leicester, UK*

Correspondence
Jonathon M Willets, Reproductive Sciences Section, Department of Cancer Studies and Molecular Medicine, University of Leicester, Clinical Sciences Building, Leicester Royal Infirmary, Leicester LE2 7LX, UK.
E-mail: jmw23@le.ac.uk

Keywords
arrestin; anandamide; CB1 receptor; endocannabinoid; ERK

Received
1 December 2010
Revised
16 March 2011
Accepted
4 April 2011

BACKGROUND AND PURPOSE

The endocannabinoid plays vital roles in several aspects of reproduction, including gametogenesis, fertilization and parturition. However, little is known regarding the presence or role of the endocannabinoid system in myometrial function. Here the presence of the endocannabinoid system and signalling properties of cannabinoid receptors were characterized.

EXPERIMENTAL APPROACH

Components of the endocannabinoid system were identified using qRT-PCR, immunohistochemical, immunoblotting and radioligand binding experiments. Cannabinoid receptor signalling pathways were characterized using standard MAPK and second messenger assays.

KEY RESULTS

Primary myometrium expresses the endocannabinoid synthesizing enzyme *N*-acyl-phosphatidyl ethanolamine-specific phospholipase D, endocannabinoid degrading enzyme fatty acid amide hydrolase and cannabinoid CB_1, but not CB_2 receptors or transient receptor potential vanilloid-type-1 channels. The CB_1 receptor ligand anandamide caused a $G\alpha_{i/o}$-dependent inhibition of adenylate cyclase reducing intracellular cAMP levels, and $G\alpha_{i/o}$, phosphoinositide-3-kinase, Src-kinase-dependent ERK activation. CB_1 receptor-generated signals declined following continual anandamide stimulation, possibly due to ligand metabolism since free anandamide concentrations declined during the experiment from 2.5 μM initially, to 500 nM after >30 min. However, identical loss of CB_1 receptor responsiveness occurred in the presence of the metabolically stable derivative methanandamide. Moreover, RNAi-mediated depletion of arrestin3 (a negative regulator of receptor signalling) prevented loss of CB_1 receptor activity, enhancing and prolonging ERK signals.

CONCLUSIONS AND IMPLICATIONS

The myometrium has the capacity to synthesize, respond to and degrade endocannabinoids. Furthermore, reduced CB_1 receptor responsiveness occurs as a consequence of receptor desensitization, not agonist depletion and we identify a key role for arrestin3 in this process.

Abbreviations

AC, adenylate cyclase; AEA, anandamide; 2-AG, 2-arachidonoylglycerol; FAAH, fatty acid amide hydrolase; GRK, G-protein coupled receptor kinase; LY294002, 2-morpholin-4-yl-8-phenylchromen-4-one; pERK, phosphorylated extracellular signal-regulated kinase; NAPE-PLD, *N*-acyl-phosphatidyl ethanolamine-specific phospholipase D; PI3K, phosphoinositide-3-kinase

Introduction

The endocannabinoid system consists of a diverse array of endocannabinoid ligands, their targets, such as the two G-protein coupled cannabinoid receptors (CB_1 and CB_2; channel and receptor nomenclature follows Alexander *et al.*, 2009) and the transient receptor potential vanilloid-type-1 (TRPV1) channel (Taylor *et al.*, 2007; Maccarrone, 2009), and the enzymes for their synthesis and degradation (Taylor *et al.*, 2010). It is however, interesting to note that endocannabinoids are also able to mediate their effects through alternative signalling pathways (O'Sullivan, 2007). Endocannabinoids are unsaturated bioactive fatty acid amides and esters, with multiple signalling roles in different tissues, controlling a plethora of physiological processes as diverse as neuronal development, inflammation, energy metabolism and reproduction (Bambang *et al.*, 2010; Taylor *et al.*, 2010). The two most studied endocannabinoids are *N*-arachidonylethanolamine (anandamide, AEA) and 2-arachidonoylglycerol (2-AG), with quantified levels of 2-AG reportedly 10-fold greater than AEA in human tissues (Taylor *et al.*, 2010). Many other bioactive endocannabinoids have recently been identified including *O*-arachidonoylethanolamine (virodhamine), *N*-arachidonoyl dopamine and *N*-acyl taurines (Bisogno *et al.*, 2000). Furthermore, several related compounds such as oleoylethanolamide (OEA) and palmitoylethanolamide (PEA) display endocannabinoid properties by inhibiting endocannabinoid catabolism or reducing cellular uptake of other endocannabinoids (Taylor *et al.*, 2010).

Endocannabinoids are synthesized as and when required from membrane lipid precursors. AEA being created through the action of *N*-acyl transferase (NAT), *N*-acyl-phosphatidyl ethanolamine-specific phospholipase D (NAPE-PLD), while 2-AG is thought to be predominantly synthesized via the conversion of diacylglycerol (DAG) through the action of *sn*-1-DAG lipase (DAGL). The bioactivity of endocannabinoids is terminated through their degradation, with AEA predominantly being metabolized by fatty acid amide hydrolase (FAAH) and 2-AG via monoacylglycerol lipase (Taylor *et al.*, 2010). However, endocannabinoids can be metabolized by many other enzymes including COXs, which can result in the production of a plethora of other bioactive compounds with diverse bioactivities (Vandevoorde and Lambert, 2007).

Accumulating evidence suggests that components of this system including endocannabinoid ligands such as AEA (although a similar role for other endocannabinoids such as 2-AG cannot be discounted) are important in the regulation of successful reproduction (Taylor *et al.*, 2007; Maccarrone, 2009). Indeed, plasma levels of AEA fluctuate throughout the menstrual cycle, being higher in the follicular than luteal phase (El-Talatini *et al.*, 2009a,b). Plasma AEA levels also fluctuate throughout pregnancy, falling in the late first and early second trimesters, prior to a fourfold increase during active labour (Habayeb *et al.*, 2004). High AEA levels have been implicated in early pregnancy loss (Maccarrone *et al.*, 2000; Habayeb *et al.*, 2008), and enhanced CB_1 receptor expression together with very low FAAH expression were identified in placental tissue from patients who underwent spontaneous miscarriage (Trabucco *et al.*, 2009). AEA also has well-defined roles in pre- and peri-implantation (Wang *et al.*, 2006a), gestation (Wenger *et al.*, 1997) and uterine relaxation (Dennedy *et al.*, 2004). Additionally, the balance of AEA signalling, or AEA 'tone', appears important in fertility and embryo implantation (El-Talatini *et al.*, 2009b). Collectively, these findings suggest that the tight regulation of the endocannabinoid system and CB receptors signalling is pivotal to successful reproductive physiology.

AEA binds to, and activates CB_1 and CB_2 receptors, which have been detected throughout the human reproductive tract, including the oviduct, uterus (Paria *et al.*, 1995) and placenta (Park *et al.*, 2003). CB_1 receptor mRNA has also been detected in the myometrial layer of the pregnant human uterus, where AEA mediates a CB_1 receptor-dependent acute myometrial relaxation (Dennedy *et al.*, 2004). Moreover, AEA dependent signalling in the immortalized human ULTR myometrial cell line is mediated through CB_1, with an absence of CB_2 receptors (Brighton *et al.*, 2009). In ULTR cells, CB_1 receptors couple to $G\alpha_{i/o}$-proteins inhibiting adenylate cyclase (AC) activity, reducing intracellular cAMP levels (Brighton *et al.*, 2009). In addition, AEA-stimulated CB_1 receptor signalling leads to ERK1/2 activation through a $G\alpha_{i/o}$-, phosphoinositide-3-kinase (PI3K)-, Src-dependent, Ca^{2+}-independent mechanism in ULTR cells (Brighton *et al.*, 2009). Collectively, these findings suggest that endocannabinoid signalling may play an important role in modulating myometrial function. Despite our previous study examining AEA signalling in ULTR (Brighton *et al.*, 2009), and a previous report detailing a CB_1 receptor-mediated relaxation of the myometrium (Dennedy *et al.*, 2004), very little is currently known about the role of the endocannabinoid system or consequences of CB receptor signalling within the myometrium. In this study we have characterized the endocannabinoid system in human myometrial cells. Furthermore, CB receptor signalling pathways, including AC inhibition, ERK1/2 activation and CB receptor desensitization, have been characterized.

Methods

Tissue collection

All protocols for human tissue collection and experimental use were approved by the University Hospitals of Leicester R&D, and the Leicestershire, Northamptonshire, and Rutland Research Ethics Committees (Reference Number 06/Q2501/48). All tissue donors gave signed informed consent and were between 30 and 48 years (mean 39 ± SD 5.8) of age. Uterine samples were obtained at hysterectomy from non-pregnant pre-menopausal women undergoing surgery for non-neoplastic indications, for example, dysfunctional uterine bleeding.

Isolation and culture of primary myometrial cells

Isolation of myometrial smooth-muscle cells. Tissue samples of myometrium measuring approximately 1 cm^3 were obtained from the myometrial muscle layer of hysterectomy samples. The myometrium was dissected free of the endometrium, serosal surfaces and any attached vaginal or cervical tissue, before washing in PBS and diced into small <1 mm^3 pieces. Myometrial cells were dissociated by enzymatic digestion of

the extracellular matrix with 50 mg·mL^{-1} collagenase (Sigma, Poole, UK), with agitation for 3 h at 37°C. Cells were collected by centrifugation and resuspended in Dulbecco's minimal essential medium (Invitrogen, Paisley, UK), then washed a further twice by repeated centrifugation and resuspension before culture.

Cell culture. Cells were routinely cultured in 75 cm^2 flasks in Dulbecco's minimal essential medium, supplemented with 10% fetal calf serum, penicillin (100 units·mL^{-1}), streptomycin (100 μg·mL^{-1}) and amphotericin B (2.5 μg·mL^{-1}), under humidified conditions at 37°C, in air/5% CO_2 and for no more than five passages.

qRT-PCR

Cells were harvested and immediately homogenized in 1 mL TRI reagent solution (Applied Biosystems) using an Ultra Turrax homogenizer on full power for 30 s on ice. RNA was extracted using 1-bromo-3-chloro-propane (Sigma, Dorset, UK) as previously described (Chomczynski and Mackey, 1995). RNA yield was determined using a Nano Drop ND1000 spectrophotometer. Ratios 260 nm/280 nm were between 1.89 and 2.04. The RNA (2 μg) was reverse transcribed (High Capacity RNA-to-cDNA kit, Applied Biosystems) and cDNA stored at –80°C. Primers for CB_1, CB_2 receptors, NAPE-PLD, FAAH, TRPV1 and β-actin were designed using Primer Express software (Applied Biosystems, Warrington, UK). cDNA was then diluted 1:10 with RNase-free water and 10 ng used for qRT-PCR using SYBR Green Master Mix (ROX) (Roche Diagnostics GmbH, Mannheim, Germany) and was performed on an ABI PRISM 7000 real-time PCR System (Applied Biosystem, Warrington, UK).

Immunohistochemical detection of endocannabinoid system

Myometrial biopsy samples were fixed immediately in 10% formal saline, embedded in paraffin and 4 μm sections mounted onto glass microscope slides coated with Vectabond tissue adhesive (Vectorlabs, Peterborough, UK) and dried for 7 days at 37°C prior to use. Sections were dewaxed in xylene (three times for 3 min) and rehydrated in graded alcohol for 3 min each and finally washed in distilled water. Sections were incubated with proteinase K (0.1 mM, Sigma, Dorset, UK) prepared in TBS buffer (Tris-base 20 mM, NaCl 149 mM, pH 7.5) at 37°C. After 1 h, tissue sections were incubated with H_2O_2 (6%) for 10 min to suppress endogenous peroxidase activity and then washed for 5 min in excess distilled water. Non-specific protein binding sites were blocked by the inclusion of goat serum diluted in TBS/0.05% v/v Tween 20. Vectastain blocking serum was added to block endogenous avidin and biotin sites according to the manufacturer's protocol. Primary antibodies against NAPE-PLD or FAAH (both from Cayman Chemical Company, Ann Arbor, MI) diluted in TBS/Tween 20 (0.05%) were applied and incubated overnight at 4°C in a humid chamber. After washing with TBS/0.1% (v/v) BSA for 20 min, slides were incubated in secondary antibody for 30 min at room temperature. Following washing with TBS/0.1% BSA for 20 min, ABC Elite (Vector) reagent was applied according to the manufacturer's instructions. After washing in TBS/0.1% BSA for 20 min slides were incubated with 3,3′-diaminobenzidine for 5 min to visualize immunostaining. Sections were then washed in running water (5 min) prior to counter-staining with Mayer's haematoxylin (Sigma, Dorset, UK), washed in running tap water for 5 min and dehydrated in graded alcohols (5 min each treatment) before clearing in xylene and mounting in butyl phthalate xylene (DPX) mounting medium (Sigma, Dorset, UK). For both antibodies, pre-absorbed controls were included using peptides (from Cayman Chemical Company, Ann Arbor, MI) according to the manufacturer's instructions.

Western blotting detection of NAPE-PLD and FAAH

Primary cultures of human myometrial cells were grown to confluency in six-well plates and lysed with modified radioimmunoprecipitation assay buffer (150 mM NaCl, 1% IGEPAL CA-630, 0.1% SDS, 50 mM Tris pH 8.0, 500 μM PMSF, 0.1 mg·mL^{-1} leupeptin, 0.2 mg·mL^{-1} benzamidine and 0.1 mg·mL^{-1} pepstatin) before addition of an equal volume of Laemmeli sample buffer (Bio-Rad, Hemel Hempstead, UK) containing β-mercaptoethanol (5% v/v). Samples were subjected to SDS-PAGE separation and Western transfer, before incubation with anti-FAAH (Cayman Chemical Company, Ann Arbor, MI, USA) or anti-NAPE-PLD (Abcam, Cambridge, UK). Immune-reactive bands were visualized using HRP-conjugated anti-rabbit secondary antibody (Sigma, Poole, UK), ECL reagent and Hyperfilm (GE Healthcare, Little Chalfont, UK).

[^{3}H]-CP55940 binding

Membrane preparation. Confluent primary human myometrial cell monolayers were dissociated in harvesting buffer (composition: HEPES 10 mM, NaCl 0.9%, EDTA 0.2%, w/v), collected by centrifugation (1000× *g*; 2 min; 4°C) and resuspended in homogenization buffer (composition: 50 mM Tris-HCl, 2.5 mM EDTA, 5 mM $MgSO_4$, pH 7.4 with KOH). Cells were homogenized and centrifuged (20 000× *g*; 4°C; 15 min) before pellets were resuspended in homogenization buffer (Lowry *et al.*, 1951). Membranes were used on the day of harvest.

Saturation binding. Experiments were performed in assay buffer (homogenization buffer with the inclusion of 1 mg·mL^{-1} BSA) in 500 μL volumes containing 100 μg cell membrane and [^{3}H]-CP55940 (PerkinElmer Life Sciences, Cambridge, UK), at concentrations ranging from 1 to 5000 pM. Non-specific binding was determined using 100 μM AEA. After 1 h at 30°C, membranes were harvested by addition of ice-cold assay buffer and filtration through 0.5% polyethylenimine pre-soaked Whatman GF/B filters. Recovered radiation was determined by standard liquid scintillation counting. Specific binding was determined as total binding minus non-specific binding.

Competition binding. Experiments were performed as above, with the exception that a saturating concentration of [^{3}H]-CP55940 was displaced by either 100 μM AEA, or varying concentrations of either the CB_1 receptor-selective agonist arachidonyl-2-chloroethylamide (ACEA) or the CB_2 receptor-selective agonist L759656. The displaced binding values

obtained for ACEA or L759656 were expressed as a percentage of those obtained with 100 μM AEA.

Inhibition of cAMP accumulation

Cell monolayers were washed with 1 mL Krebs-HEPES buffer (HEPES; 10 mM, $NaHCO_3$; 1.3 mM, D-glucose; 11.7 mM, $MgSO_4 \cdot 7H_2O$; 1.2 mM, KH_2PO_4; 1.2 mM, KCl; 4.7 mM, NaCl; 118 mM, $CaCl_2 \cdot 2H_2O$; 1.3 mM, pH 7.4) and incubated at 37°C for 10 min in 1 mL of Krebs-HEPES buffer. Cells were pre-treated with the phosphodiesterase (PDE) inhibitor IBMX (300 μM) for 10 min before treatment with varying concentrations of AEA for 10 min for dose–response experiments. cAMP was then raised by a 10 min treatment with forskolin (10 μM). For desensitization experiments cells were treated in an identical manner, except that cells were pre-incubated with AEA (10 μM) for various time periods prior to inclusion of forskolin (10 μM, 10 min). Samples were neutralized and cAMP concentrations determined by radioligand binding assay as described previously (Brown *et al.*, 1971).

Detection of AEA-stimulated ERK1/2 phosphorylation

Detection of phospho-(p)ERK and total ERK1/2 was undertaken as described previously (Brighton *et al.*, 2009). Briefly, cells were grown to confluency in six-well plates for 24 h, and serum-starved for a further 24 h before assay. Cells were washed in Krebs-HEPES buffer (composition as above). Next, cells were either treated with inhibitors for various time periods, stimulated with 10 μM AEA or other test agents. After agonist challenge, cells were lysed, subjected to SDS-PAGE separation and Western transfer, and pERK1/2 levels were determined using an anti-pERK1/2 antibody (Promega, Southampton, UK), before visualization using HRP-conjugated anti-rabbit secondary antibody (Sigma, Poole, UK), ECL reagent and Hyperfilm (GE Healthcare, Little Chalfont, UK). The relative levels of pERK1/2 were determined using the GeneGnome image analysis system and software (Syngene, Cambridge, UK). To ensure all gels were equally loaded for protein, membranes were subsequently stripped and reprobed for total ERK1/2 using a specific anti-ERK1 antibody (Santa Cruz, CA). Immunoreactive bands were visualized and quantified as described above. pERK1/2 absorbance levels for each treatment were corrected for differences in total ERK1/2 immunoreactivity before being expressed as a percentage of the basal pERK1/2 immunoreactivity.

siRNA targeted arrestin depletion

To assess the involvement of endogenous arrestins in the regulation of CB receptor signalling primary myometrial cells were transfected with anti-arrestin siRNAs using the Lonza nucleofection technique (Lonza, Gaithersburg) according to the manufacturer's optimized protocol (Willets *et al.*, 2008). Briefly, 1×10^6 cells per reaction were transfected with various concentrations of either anti-arrestin2 (5′-GGAGAUCUAUUACCAUGGAtt-3′), anti-arrestin3 (5′-CGAACAAGAUGACCAGGUAtt-3′) or negative-control siRNAs, prior to seeding onto six-well plates. After 48 h, cells were lysed and subjected to electrophoretic separation as described previously (Willets and Kelly, 2001). Separated proteins were transferred to nitrocellulose and arrestin expression detected using a polyclonal antibody raised against arrestin2 (A1CT), which also detects arrestin3, albeit at lower affinity, enabling visualization of both arrestins on one blot (Ahn *et al.*, 2003). Protein expression was visualized after application of HRP-conjugated anti-rabbit secondary antibody (Sigma, Poole, UK), ECL reagent and exposure to Hyperfilm (GE Healthcare, Little Chalfont, UK). The relative expression of individual arrestin proteins was determined using the GeneGnome image analysis system and software (Syngene, Cambridge, UK).

Measurement of AEA concentrations

To examine the stability of AEA in contact with myometrial cells during long incubation periods, the concentration of AEA was determined at various times, using our established UPLC-ESI-MS/MS technique (Lam *et al.*, 2008). Briefly, cells were exposed to AEA (10 μM) for various time periods during CB_1 receptor desensitization experiments. At the end of each period, samples (10 μL) of standard Krebs buffer were taken, 10 μL of AEA-d8 (as internal standard) in acetonitrile (125 pM) added, and then more acetonitrile (20 μL). Samples were then vortex mixed and then kept at –20°C for 5 min to precipitate protein, centrifuged for 1 min at 10 000× *g*, before the supernatant was transferred to a HPLC vial for AEA determination via UPLC-ESI-MS/MS.

Data analysis

All data shown are expressed as the mean of at least three experiments (unless otherwise stated) ± SEM. Concentration–response curves were fitted using Prism version 5.0 (GraphPad Software Inc., San Diego, CA). Data were analysed using one-way or two-way ANOVA, followed by appropriate *post hoc* testing (Excel 5.0, Microsoft, Redmond, WA). Significance was accepted when $P < 0.05$. Saturation radioligand binding data were fitted using Prism version 5.0 and the B_{max} and PK_D values were obtained from these graphs. For displacement analysis, graphs were again fitted using Prism 5.0, and IC_{50} values obtained. The pK_i value was determined from these data according to the Cheng–Prusoff equation (Cheng and Prusoff, 1973) where $K_i = IC_{50}/(1 + [^3H]\text{-CP55940}/K_D)$. Here the average K_D value obtained from our three separate saturation experiments was used.

Materials

Compounds used in these experiments were obtained as follows; ACEA, AM251, CP55940, L75956, PP1 and LY294002 were from Tocris (Bristol, UK) and AEA from Ascent Scientific (Bristol, UK). Forskolin, IBMX, URB597, methanandamide were supplied by Sigma Aldrich (Poole, UK) and AEA-(d8) was from Cayman Chemicals (Ann Arbor, MI, USA). Piroxicam was a kind gift from Dr. Stewart Sale, University of Leicester.

Results

Characterization of the endocannabinoid system in primary myometrial cells

A multi-experimental approach was applied to determine which components of the endocannabinoid system are

Table 1

Quantitative RT-PCR characterization of the myometrial endocannabinoid system

	CB_1	CB_2	TRPV1	FAAH	NAPE-PLD	β-Actin
Cell type	Ct	Ct	Ct	Ct	Ct	Ct
ULTR	11.2 ± 0.43	16.7 ± 0.13	9.2 ± 0.40	15.4 ± 0.94	9.5 ± 0.24	16.8 ± 0.15
Primary	16.1 ± 0.49	17.5 ± 0.21	11.2 ± 0.26	17.1 ± 0.51	10.1 ± 0.05	17.6 ± 0.35

Mean cycle threshold (Ct) values for CB_1 and CB_2 receptors, TRPV1 channels, FAAH, NAPE-PLD and β-actin in ULTR and primary myometrial cells. Samples were assayed in triplicate from three separate extractions from $n = 3$ separate patients and expressed as mean Ct values ± SEM. cDNA from ULTR and primary myometrial cell lysates were amplified with specific, commercially verified, primer/probe sets. All data are related to ΔRn; the change in the normalized reporter fluorescence, relative to basal.

present in the human myometrium. Initially, we utilized qRT-PCR techniques to determine whether myometrial cells expressed mRNA transcripts for FAAH, NAPE-PLD, TRPV1 and CB_1 receptors. Our data indicate the presence of NAPE-PLD, FAAH, CB_1 receptor and TRPV1 transcripts in myometrial cells (Table 1). As mRNA levels are not always reflective of protein expression levels we undertook immunoblotting experiments to confirm the presence of NAPE-PLD and FAAH proteins (Figure 1A). Furthermore, immunocytochemical studies also demonstrated the presence of NAPE-PLD and FAAH expression in myometrial biopsy samples (Figure 1B–G). Despite the presence of TRPV1 transcripts in both primary myometrial and ULTR cells, TRPV1 protein expression was not detectable by immunoblotting (data not shown). In addition, intracellular calcium levels were unaltered following stimulation with either the TRPV1 agonist capsacin or AEA (data not shown), which suggests an absence of the TRPV1 channels in myometrial cells.

Determination of relative CB_1 and CB_2 receptor expression in primary myometrial cells

Due to the lack of appropriate high-quality commercially available antibodies for CB receptors (Grimsey *et al.*, 2008), the potential expression of CB_1 and CB_2 receptors was determined by investigating the binding properties of the non-selective cannabinoid receptor agonist [^{3}H]-CP55940 to cell membranes prepared from human primary cultured myometrial smooth-muscle cells. [^{3}H]-CP55940 binding was saturable (see insert Figure 2A), and the specific component, as determined by inclusion of 100 μM AEA, represented approximately 15% of the total binding observed at K_D concentrations of [^{3}H]-CP55940 (data not shown). The B_{max} and pK_D values were obtained following full saturation analysis of specific binding and were 52.7 ± 6.9 fmol·mg protein^{-1}, and 9.53 ± 0.26 (295 pM) respectively (Figure 2A, data are mean ± SEM, $n = 5$). To determine the relative expression of CB_1 and CB_2 receptors in membrane preparations, saturable concentrations of [^{3}H]-CP55940 were displaced by agonists that selectively target either CB_1 and CB_2 receptors. Inclusion of the CB_1 receptor selective agonist arachidonyl-2-chloroethylamide (ACEA) completely displaced specific [^{3}H]-CP55940 binding, with full concentration analysis revealing a pIC_{50} value of 7.24 ± 0.17 (IC_{50} 57 nM), and following Cheng–Prusoff (Cheng and Prusoff, 1973) correction, a K_i of –7.44 ± 0.12 (36 nM) (Figure 2B, data are mean ± SEM, $n = 5$). To ascertain the CB_2 receptor component, saturable concentrations of [^{3}H]-CP55940 were displaced by the CB2 selective agonist L759656. L759656 has a 428-fold selectivity for CB_2 receptors (reported K_i values were 4.9 μM and 11.8 nM for CB_1 and CB_2 receptors respectively) (Ross *et al.*, 1999), and only displaced [^{3}H]-CP55940 binding at concentrations above 1 μM. At these concentrations L759656 displaced approximately 10–20% specific [^{3}H]-CP55940 binding. These observations suggest that displacement was as a result of cross-reactivity of L759656 with the CB_1 receptor, suggesting an absence of CB_2 receptors in these cells. Analysis of these data would therefore indicate that CB_1 receptors were responsible for all AEA-mediated signalling events within our human cultured primary myometrial smooth muscle cells.

Characterization of AEA-stimulated ERK1/2 phosphorylation

Incubation with AEA resulted in time-dependent increases in ERK1/2 phosphorylation (Figure 3), which peaked 15 min after adding AEA (10 μM) and slowly declined over the following 60 min (Figure 3A,B). Concentration–response data (Figure 3C,E) undertaken 15 min after AEA incubation revealed maximal ERK1/2 phosphorylation at >10 μM with pEC_{50} values of 6.0 ± 0.44 (EC_{50} 1 μM) (data are mean ± SEM, $n = 4$). The metabolically stable AEA analogue methanandamide (Abadji *et al.*, 1994) produced a more potent ERK1/2 phosphorylation with pEC_{50} values of 6.89 ± 0.21 (EC_{50} 128 nM) (data are mean ± SEM, $n = 4$; Figure 3D,E). To characterize the cellular events that link AEA-mediated CB_1 receptor activity to the phosphorylation of ERK1/2, we examined the effects of a series of inhibitors, specifically targeting cellular proteins and enzymes acting downstream of GPCRs and known to be involved in ERK1/2 signalling. Pre-treatment of cells with the $G\alpha_{i/o}$ inhibitor, *Pertussis* toxin (PTX; 100 ng·mL^{-1}, 20 h) abolished all AEA-mediated ERK1/2 phosphorylation (Figure 4A,E), suggesting that CB_1 receptor activation and coupling through its effector G-protein is essential. Similar results were observed following inhibition of PI3K (30 min pre-treatment with 100 nM

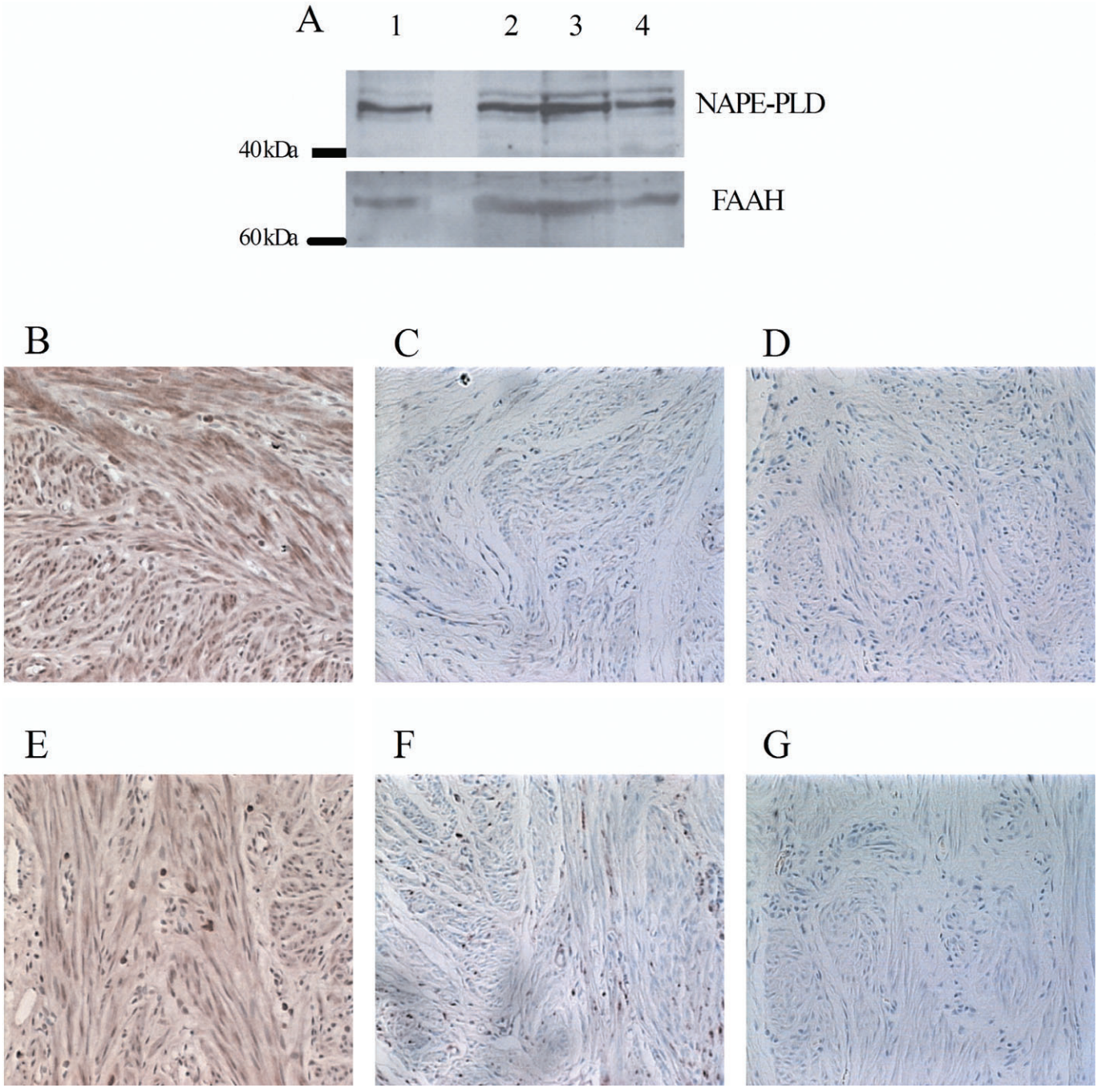

Figure 1

Characterization of the myometrial endocannabinoid system. (A) Representative immunoblots show NAPE-PLD (predicted 46 kDa) and FAAH (predicted 67 kDa) expression in ULTR (lane 1), and primary myometrial cell lysates from three separate patient donors (lanes 2–4). Myometrial biopsies were formalin-fixed and processed into paraffin blocks. Slides were then cut and stained for NAPE-PLD and FAAH using standard immunohistochemical techniques. Representative images are shown depicting NAPE-PLD (B) and FAAH (E) staining. Pre-absorbed controls using 1:10 dilution of blocking peptide (C and F), and isotype IgG controls (D and G) are shown for NAPE-PLD and FAAH antibody staining respectively.

LY294002) (Figure 4B,E) and the non-receptor tyrosine kinase Src (30 min pre-treatment with 5 μM PP1) (Figure 4C,E). In addition, inclusion of the CB_1 receptor selective antagonist AM251 (15 min pre-treatment with 1 μM) also abolished AEA-stimulated ERK1/2 phosphorylation (Figure 4D,E). Our findings are in agreement with those obtained in ULTR cells (Brighton *et al.*, 2009), and further emphasizes the similarities between these cell types.

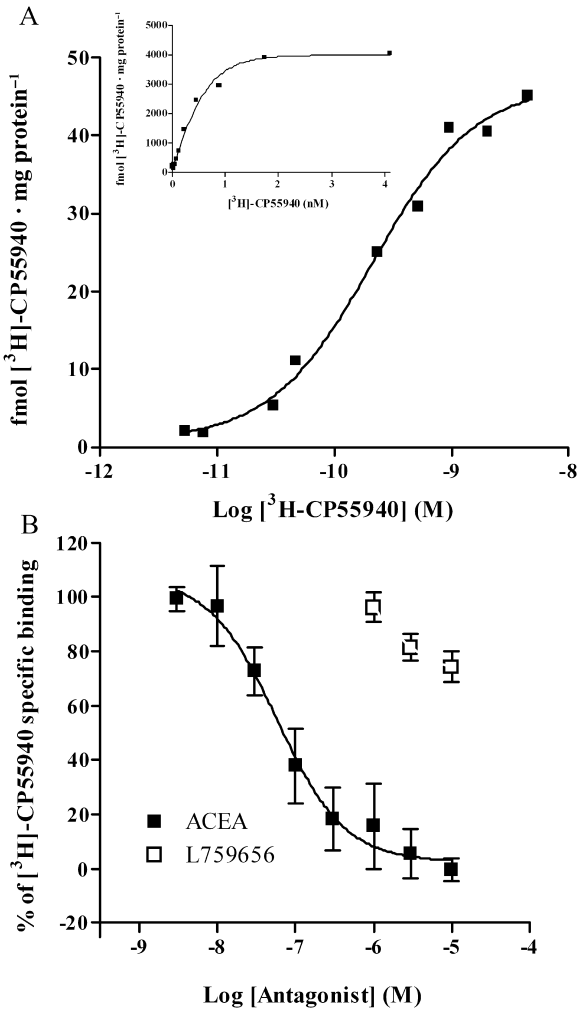

Figure 2

Expression of CB_1 and CB_2 receptors by radioligand binding. Cell membranes (100 μg) were incubated with [^{3}H]-CP55940 and various CB receptor agonists for 1 h at 30°C, before filtration through 0.5% polyethylenimine pre-soaked Whatman GF/B filters. Associated [^{3}H] was determined by standard liquid scintillation counting. (A) Saturation analysis. Cell membranes were incubated with varying concentrations of [^{3}H]-CP55940 ranging from 1 to 5000 pM either in the presence (non-specific binding) or absence (total binding) of 100 μM AEA. Non-specific binding values were subtracted from total binding and plotted graphically in relation to protein. B_{max} and K_i values obtained were 52.7 ± 6.9 fmol·mg protein^{-1}, and –9.53 ± 0.26 (~295 pM) respectively. Data are mean ± SEM, $n = 5$ membrane preparations from five separate patient donors. The insert shows specific binding in a non-log format to show saturation of [^{3}H]-CP55940 more clearly. (B) Displacement of [^{3}H]-CP55940 using CB_1 and CB_2 receptor specific agonists. Cell membranes were incubated with saturating concentrations of [^{3}H]-CP55940 in the presence of either 100 μM AEA, or varying concentrations of ACEA (CB_1 receptor-selective agonist) or L759656 (CB_2 receptor-selective agonist) ranging from 10 nM to 10 μM. Specific binding values obtained for each concentration of ACEA and L759656 are expressed as a percentage of those obtained with 100 μM AEA. The pK_i value obtained for ACEA was 7.24 ± 0.17 (IC_{50} 57 nM), and following Cheng–Prusoff correction (Cheng and Prusoff, 1973), a pK_i of 7.44 ± 0.12 (36 nM). Data are mean ± SEM, $n = 5$ membrane preparations from five separate patient donors.

Characterization of AEA-stimulated, CB_1 receptor-mediated inhibition of AC signalling and receptor desensitization

To investigate CB_1 receptor signalling through AC in primary myometrial cells we investigated the ability of AEA to inhibit forskolin (10 μM)-stimulated cAMP accumulation. Following treatment of cells with the PDE inhibitor IBMX, mean basal levels of cAMP were 51 pmol·mg protein^{-1}, while forskolin (10 μM, 10 min) addition increased cellular cAMP accumulation to 2900 ± 209 pmol·mg protein^{-1} (data means ± SEM, for $n = 6$, experiments from cells prepared from six patients). Initial experiments indicated that AEA induced a concentration-dependent inhibition of the cAMP production generated by forskolin, with maximal inhibition observed at AEA concentrations above 10 μM and pIC_{50} values of 6.64 ± 0.28; 229 nM; (data are means ± SEM, $n = 4$). Furthermore, pre-incubation with the CB_1 receptor-selective antagonist AM251 completely reversed the ability of AEA to inhibit forskolin-stimulated cAMP accumulation (Figure 5A).

Usually GPCR desensitization experiments compare responses generated in the presence or absence of agonist pre-treatment. However, due to the hydrophobic nature of CB receptor ligands combined with the subsequent inability to completely remove them from experiments, we established a different desensitization protocol. Here cells were exposed to AEA (10 μM) for varying pre-incubation time periods prior to addition of the AC activator, forskolin (10 μM, for 10 min), with vehicle pre-treated cells used as controls. With no pre-incubation period, AEA inhibited forskolin-stimulated cAMP production by ~80% (Figure 5A). A similar level of AC inhibition was observed with AEA pre-incubation periods of up to 10 min. Nevertheless, the effectiveness of AEA to inhibit AC activity gradually declined with increasing pre-incubation periods (>15 min) until no inhibition was observed after pre-incubation for more than 45 min (Figure 5B). AEA like all endocannabinoid molecules is subject to enzymatic (by FAAH, COX) and other forms of degradation, which may underlie the loss of receptor responsiveness observed during desensitization experiments. Consequently we firstly repeated our CB_1 receptor desensitization experiments with the metabolically stable AEA analogue methanandamide (Abadji *et al.*, 1994) to exclude the effects of agonist degradation. Our initial concentration–response data indicated that methanandamide was more potent than AEA (Figure 3); therefore, concentrations of each agonist were matched to produce equipotent responses. Interestingly, the temporal profile of methanandamide (1 μM) inhibition of forskolin-stimulated cAMP production was identical to that produced by AEA (10 μM, Figure 5B). In addition, inclusion of either FAAH [URB597, 100 nM; (Kawahara *et al.*, 2010)] or COX1/2 [piroxicam, 1 μM; (Sale *et al.*, 2009)] inhibitors did not alter the temporal profile of AEA-mediated inhibition of forskolin-stimulated cAMP accumulation (Figure 5C). As AEA/CB_1 receptor-stimulated ERK phosphorylation peaked at 15 min gradually declining thereafter, returning to basal levels at 90 min, we decided to determine whether the loss of signal was possibly due to metabolic AEA degradation. In agreement with our AC data, the time-course of ERK phosphorylation was identical in the presence of AEA (10 μM) or methanan-

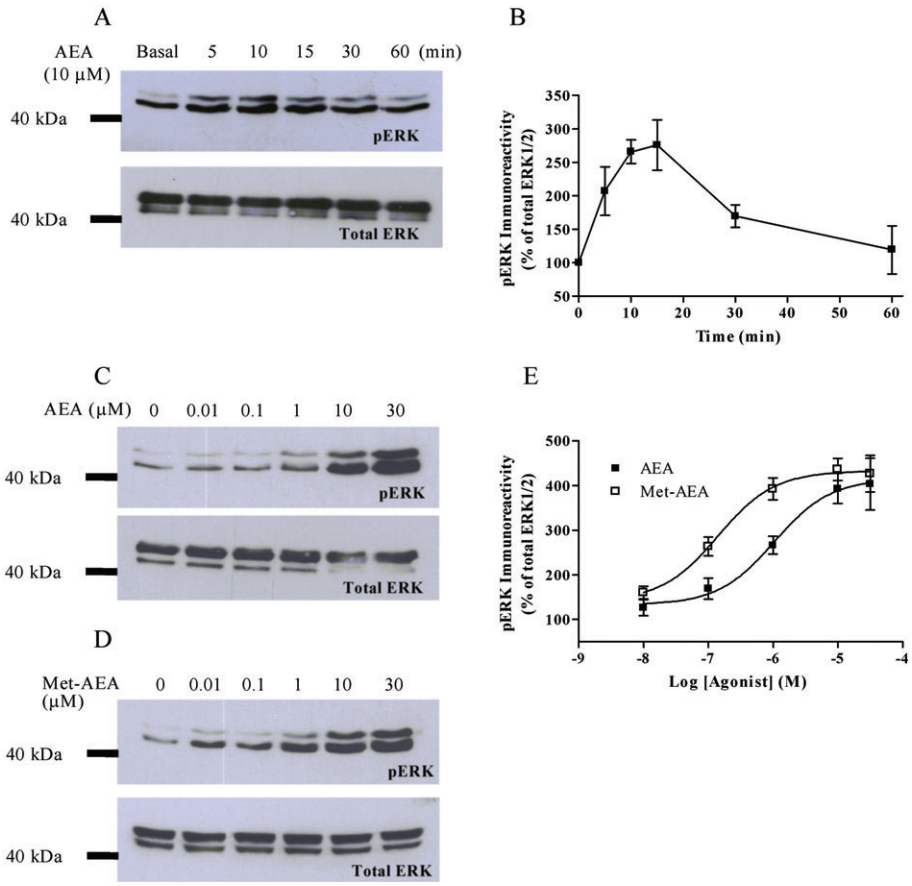

Figure 3

Time-course and concentration-dependency of AEA-mediated ERK1/2 phosphorylation. Cells were serum-starved for 24 h before agonist stimulation, and pERK1 (44 kDa)/2 (42 kDa) levels determined by standard immunoblotting techniques (upper panels). To verify equal gel loading all blots were stripped and reprobed with anti-ERK1 antibody (lower panels). Representative immunoblots show the time-course of AEA (10 μM) (A) and concentration-dependency of AEA and methanandamide (Met-AEA) (C and D) stimulated ERK1/2 activation. Concentration–response curves were undertaken at the peak ERK1/2 phosphorylation time period of 15 min. Cumulative densitometric analysis of pERK1/2 signals are shown for time-course (B) and concentration-dependent (E) AEA-, Met-AEA-stimulated signals. Data are means ± SEM for $n = 4$ experiments from cells prepared from four separate patient donors.

damide (1 μM, Figure 6A–C) and was not affected after addition of FAAH or COX inhibitors (Figure 6D–F).

To further determine the stability of AEA throughout desensitization experiments, samples of buffer were taken from each well at the end of all pre-incubation periods. AEA was subsequently extracted and concentrations determined using UPLC-ESI-MS/MS (Lam *et al.*, 2008). Our data show that AEA concentrations measured in the experimental buffer (with or without cells) were considerably less (i.e. 2.5 μM) than the expected 10 μM, even at the 0 min pre-incubation time point (Figure 7). As a further control, stock AEA concentrations were also analysed by UPLC-ESI-MS/MS and confirmed to contain 5.05 ± 0.09 mM (data mean ± SEM for n = 8 separate samples), which when diluted 500-fold should have yielded 10 μM in our experiments. In the presence of cells, AEA concentrations remained stable for the first 5 min before declining over the next 15 min, finally settling to a steady concentration of around 500 nM between 30 and 60 min (Figure 7). Inclusion of either the FAAH inhibitor URB597 (100 nM) or the COX inhibitor piroxicam (1 μM) prevented the decline of AEA concentrations in the presence of cells, suggesting that both enzymes contributed towards the observed depletion of free AEA.

Depletion of arrestin3 prevents CB_1 receptor desensitization

Arrestin proteins are established negative regulators of GPCR signalling (DeWire *et al.*, 2007). Therefore, to assess their roles in myometrial AEA signalling, we used a siRNA approach to target endogenous arrestin expression. To optimize endogenous arrestin protein depletion, myometrial cells were transfected with 10, 50 or 100 nM of siRNA targeting arrestin2, arrestin3 or a negative-control siRNA. Initial experiments revealed that maximal depletion of either arrestin isoform could be achieved 48 h after transfection (data not shown). Maximal arrestin2 depletion (>70%) was attained following application of >50 nM anti-arrestin2 siRNA; however, 100 nM also reduced arrestin3 expression by 30%; therefore, 50 nM was used for all other experiments (Figure 8A,C). The A1CT antibody also detects arrestin3, albeit with lower affin-

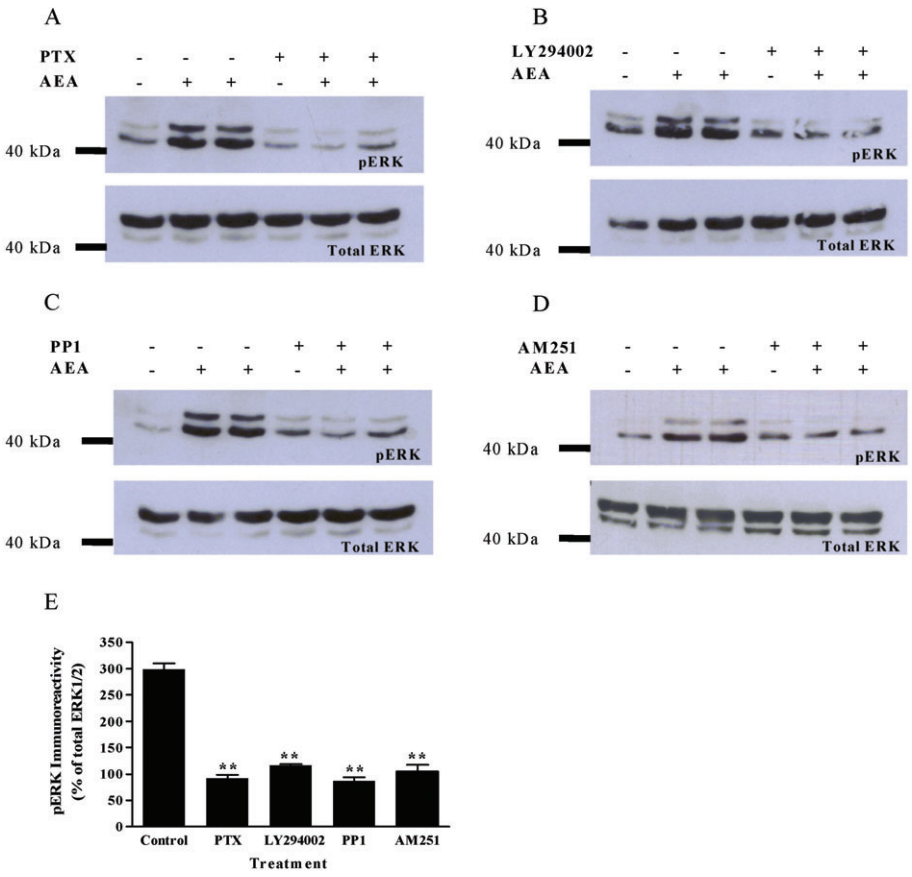

Figure 4

Identifying the signalling pathway mediating AEA-mediated ERK1/2 activation. Serum-starved cells were stimulated with AEA (10 μM) for 15 min following pre-treatment with either (A) PTX (100 ng·mL^{-1}, 20 h, $G\alpha_{i/o}$ G-protein inhibitor), (B) LY294002 (100 nM, 30 min, PI3K inhibitor), (C) PP1 (5 μM, 30 min, Src-kinase inhibitor) or (D) the CB_1 receptor-selective antagonist AM251 (1 μM, 15 min). AEA-mediated ERK1 (44 kDa)/2 (42 kDa) phosphorylation was determined by standard immunoblotting techniques (representative blots are shown: A–D, upper panels) and to verify equal gel loading all blots were stripped and reprobed with anti-ERK1 antibody (lower panels). Cumulative densitometric analysis of pERK1/2 signals are shown (E) indicating that AEA-stimulated ERK1/2 activation is mediated through CB_1 receptor, $G\alpha_{i/o}$, PI3K and Src activity. Data are expressed as means ± SEM, $n = 3$ experiments, from three separate patient donors. $^{**}P < 0.01$, significant inhibition of ERK1/2 phosphorylation (one-way ANOVA; Bonferroni's *post hoc* test).

ity, enabling visualization of both arrestins on one blot. Indeed, increased exposure of the same blot (Figure 8B,C) highlights the maximal depletion of arrestin3 expression (>80%) with concentrations of anti-arrestin3 siRNA of >10 nM with no affects upon arrestin2 expression. Crucially, negative-control siRNA had no effect upon arrestin expression (Figure 8). Having established a protocol that produced maximal depletion of endogenous arrestins, the effects of their depletion on AEA receptor signalling/desensitization was examined. Initially, the effects of arrestin suppression on CB_1 receptor desensitization were assessed at the level of cAMP. Again cells were treated with AEA (10 μM) for varying pre-incubation periods, before addition of the AC activator, forskolin (10 μM, for 10 min), with vehicle pre-treated cells used as controls. Importantly, both basal and forskolin-stimulated cAMP levels were identical following transfection with negative-control, arrestin2 or arrestin3 siRNAs (Figure 9A). In the presence of negative-control or arrestin2 siRNAs, the temporal profile of CB_1 receptor desensitization (Figure 8A) was similar to that observed in non-transfected cells (data not shown). Maximal AEA inhibition of AC activity was observed with pre-incubation periods ≤10 min, declining with longer pre-incubation until absent after 45 min pre-incubations, which suggests that CB_1 receptors were fully desensitized by this time (Figure 9A). Interestingly, suppression of arrestin3 expression totally prevented CB_1 receptor desensitization even after 60 min AEA pre-incubation (Figure 9A). For several other GPCRs, arrestin proteins not only mediate desensitization but can act as agonist-regulated adaptor scaffolds for several MAPK signalling pathways such as ERK1/2 (DeWire *et al.*, 2007). Therefore, we decided to examine whether arrestin proteins played a similar role in CB_1 receptor-stimulated phosphorylation of ERK1/2 in myometrial cells. The time-course of AEA/ CB_1 receptor-mediated ERK1/2 phosphorylation was unaltered in the presence of negative-control and arrestin2 siRNAs. However, ERK1/2 signals were markedly enhanced and prolonged following arrestin3 suppression (Figure 9C,D). Collectively,

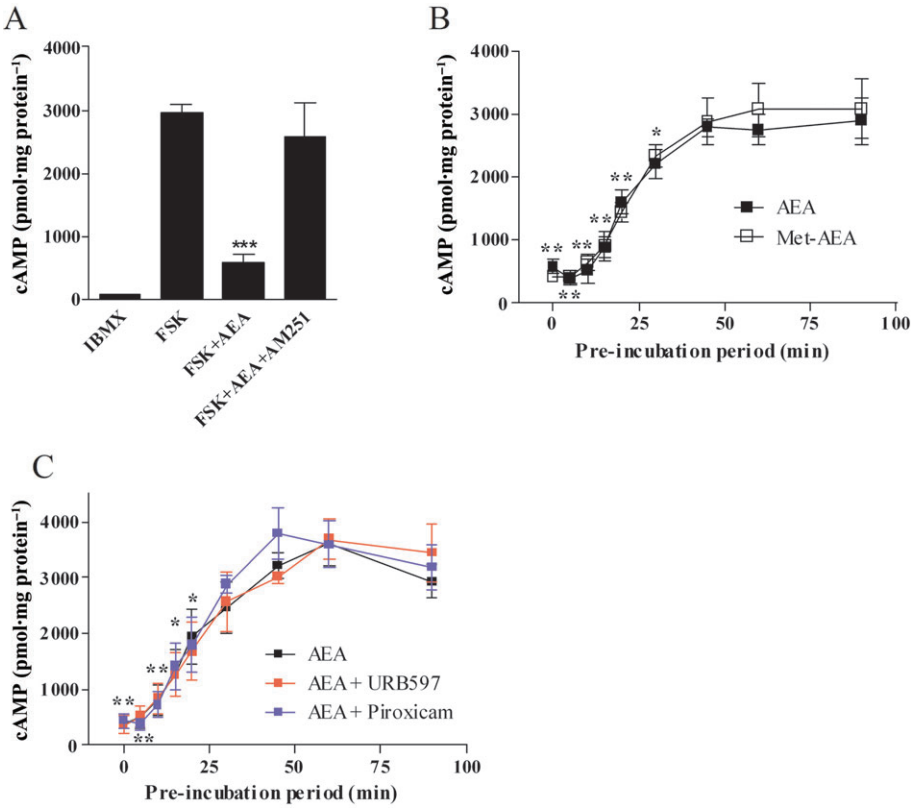

Figure 5

Characterization of CB_1 receptor desensitization. (A) Cells were treated with forskolin (10 μM, 10 min) in the presence or absence of AEA (10 μM, added at the same time as forskolin), or the CB_1 receptor-selective antagonist AM251 (1 μM, 15 min pre-treatment). After forskolin addition, cAMP accumulation was terminated with ice-cold trichloroacetic acid, before cellular cAMP was extracted, and levels determined by radioreceptor assay. Forskolin stimulated cAMP production in myometrial cells, which was inhibited by AEA (***$P < 0.001$, significantly different from forskolin and AM251 treated cells; one-way ANOVA; Dunnett's *post hoc* test), and reversed following pre-incubation with the CB_1 receptor-selective antagonist AM251 (1 μM, 15 min). (B) The time-courses of AEA- and methanandamide (Met-AEA)-mediated CB_1 receptor desensitization was examined at the level of cAMP inhibition. Primary myometrial cells were exposed to a single maximal concentration of AEA (10 μM) or Met-AEA (1 μM) for varying periods prior to addition of the AC activator forskolin (10 μM) for a further 10 min. (C) Identical experiments were undertaken in the presence of URB597 (FAAH inhibitor, 100 nM) and piroxicam (COX1/2 inhibitor, 1 μM). In both cases cAMP levels were determined as described above. Data are shown as means ± SEM for six cell preparation from six separate patient donors. *$P < 0.05$; **$P < 0.01$, significant inhibition of forskolin-induced cAMP accumulation (one-way ANOVA; Dunnett's *post hoc* test).

these observations suggest that arrestin3 plays a key role in the desensitization of CB_1 receptor signalling.

Discussion

Although marijuana use is associated with pre-term labour and prolonged gestation (Taylor *et al.*, 2007), suggesting a role for the cannabinoid system in the regulation of myometrial activation (an essential requirement for active labour), few studies have investigated the role of the endocannabinoid system in myometrial function (Dennedy *et al.*, 2004). Here we utilized a combination of approaches to characterize the presence of components of the endocannabinoid system in human myometrium. Indeed, our qRT-PCR data indicate that primary myometrial cells are capable of producing NAPE-PLD, FAAH, CB_1 receptor and TRPV1 transcripts. As the presence of mRNA transcripts does not guarantee subsequent translation, the expression of FAAH and NAPE-PLD proteins were confirmed using Western blotting in isolated cultured myometrial cells, and in whole myometrial tissues using immunohistochemistry. However, despite the presence of TRPV1 mRNA, we were unable to show the presence of functional TRPV1 channels in myometrial cells. Interestingly, the timing and rate of mRNA translation is controlled by several post-transcriptional regulatory mechanisms. For example, mRNA modification, sequence-specific nuclear export, mRNA sequestration and non-coding RNAs can all determine when and how efficiently mRNA is converted into protein. It is therefore possible that a particular mRNA could be present in the absence of the corresponding protein. Due to the lack of appropriate high-quality commercially available antibodies for CB receptors (Grimsey *et al.*, 2008), we utilized our previously validated [^{3}H]-CP55940 binding assay (Brighton *et al.*, 2009) to characterize which if any CB receptors were expressed on primary myometrial cells. Consistent with our

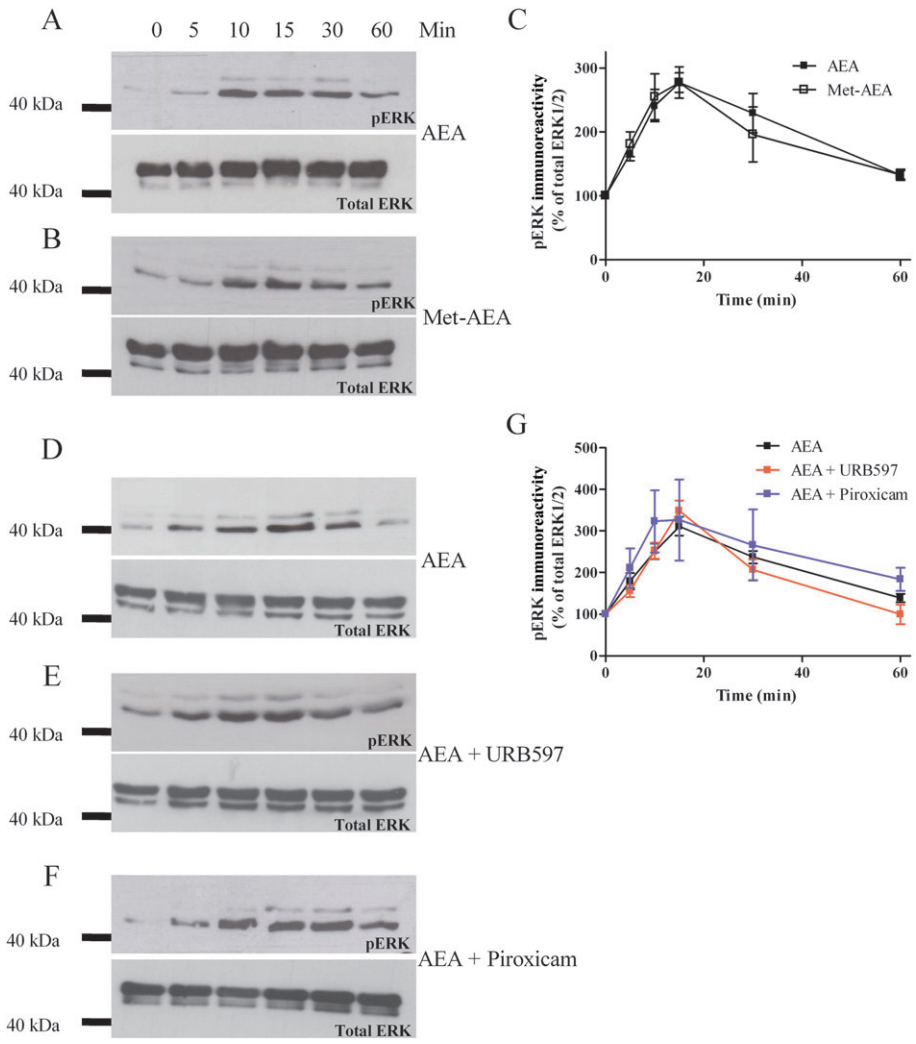

Figure 6

The time-course of ERK phosphorylation induced by AEA (10 μM) or Met-AEA (1 μM) was also examined in myometrial cells, which were serum-starved for 24 h before agonist stimulation. pERK1/2 levels were determined by standard immunoblotting techniques (upper panels). To verify equal gel loading all blots were stripped and reprobed with anti-ERK1 antibody (lower panels). Representative immunoblots show the time-course of AEA (A) and Met-AEA (B) induced ERK1 (44 kDa)/2 (42 kDa) phosphorylation. (C) Cumulative densitometric analysis of pERK1/2 signals indicated that the temporal profiles and magnitude of AEA and Met-AEA-induced ERK phosphorylation are identical. Data are expressed as means ± SEM, $n = 4$ experiments, from four separate patient donors. In D, representative immunblots are displayed showing AEA-stimulated ERK1/2 phosphorylation before and after (E) inclusion of the FAAH inhibitor URB597 (100 nM) or the COX1/2 inhibitor piroxicam (1 μM) (F). Cumulative densitometric analysis of pERK1/2 signals (G) indicated that the temporal profiles and magnitude was unaffected following FAAH or COX1/2 inhibition. Data are expressed as means ± SEM, $n = 4$–7 experiments, from four to seven separate patient donors.

previous findings in ULTR cells (Brighton *et al.*, 2009), [^{3}H]-CP55940 and antagonist competition binding data identified a predominantly CB_1 receptor population in myometrial membranes. Moreover, the CB_2 receptor ligand L759656 displaced [^{3}H]-CP55940 only at concentrations >1 μM, reflecting its affinity for CB_1 (K_D at CB1 = 4888 nM) rather than CB_2 receptors (K_D at CB2 = 11.8 nM) (Ross *et al.*, 1999). Therefore, it is unsurprising that at high L759656 concentrations (1–10 μM) inhibition of CB_1 receptor binding was observed, suggesting that AEA signalling was predominantly mediated through CB_1 receptors. Collectively, these data highlight, for the first time, the existence of many components of the endocannabinoid system in primary myometrial cells. Thus it appears that the myometrium has the capacity to synthesize (via NAPE-PLD activity), respond to (via CB_1 receptors) and degrade (via FAAH) endocannabinoids. Moreover, we have previously detected low (nM) levels of AEA in myometrial cell culture media (P.J. Brighton *et al.*, unpubl. obs.).

Considering the importance of CB_1 receptors and AEA signalling in general to successful human reproduction (Taylor *et al.*, 2010) it is surprising how little is currently known regarding the regulation of this GPCR and its signalling properties, particularly in reproductive tissues. To address this issue we examined CB_1 receptor desensitization using AC inhibition and ERK1/2 phosphorylation as indices of CB_1

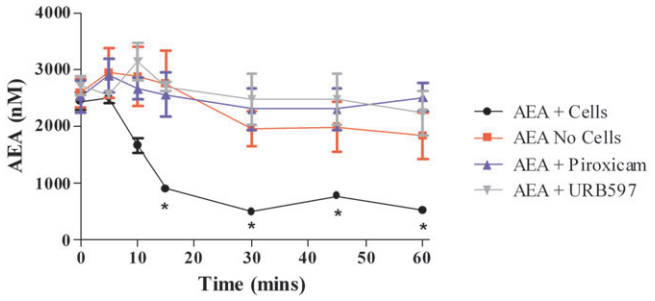

Figure 7

Time-course of free AEA concentrations in the presence or absence of cells, or following inclusion of the FAAH inhibitor URB597 (100 nM) or COX1/2 inhibitor piroxicam (1 μM). The concentration of free AEA in the experimental buffer was determined in the presence and absence of myometrial cells following addition of 10 μM AEA. Samples were taken at the indicated time points and AEA concentrations determined using UPLC-ESI-MS/MS . Data are means ± SEM for samples taken from five separate experiments, using cells prepared from five patient donors. In the presence of cells, the AEA concentrations declined rapidly and this was prevented following inclusion of FAAH or COX inhibitors. *$P < 0.05$, significantly different from values in the absence of cells; or following inclusion of URB597 or piroxicam to cells; two-way ANOVA; Bonferroni's *post hoc* test).

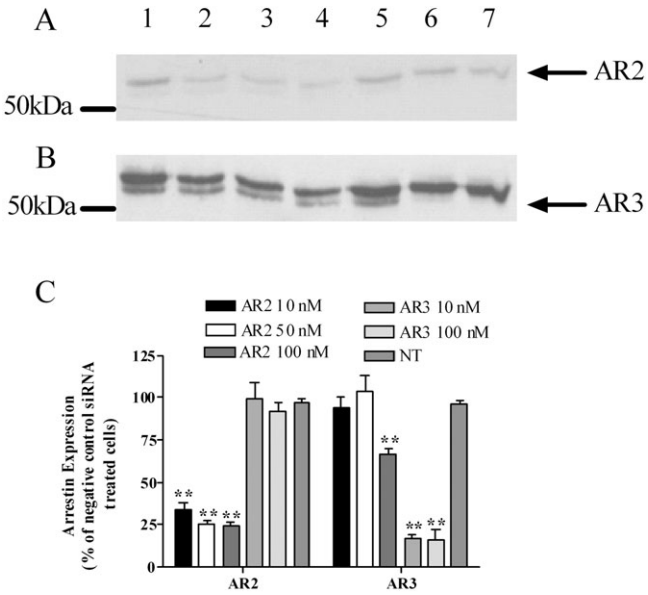

Figure 8

siRNA-mediated suppression of arrestin2 and 3 expression. Myometrial cells were transfected with various concentrations of anti-arrestin2, anti-arrestin3 or negative-control siRNAs using the Lonza nucleofection technique. After 48 h cells were lysed and arrestin expression determined using standard Western blotting techniques (as described in *Methods*). (A) Representative immunoblot showing arrestin2 (AR2; predicted weight 55 kDa) expression following treatment with lane 1: negative-control (100 nM); lane 2: anti-arrestin2 (10 nM); lane 3: anti-arrestin2 (50 nM); lane 4: anti-arrestin2 (100 nM); lane 5: non-transfected cells; lane 6: anti-arrestin3 (10 nM); or lane 7: anti-arrestin3 (100 nM) siRNAs respectively. (B) The same representative immunoblot is shown with greater exposure to visualize arrestin3 (AR3; predicted weight 50 kDa) expression (lower band). (C) Cumulative densitometric data showing the extent of siRNA-mediated arrestin suppression in myometrial cells. The relative immunoreactivity of individual arrestin bands after transfection with various concentrations of either anti-arrestin2 or anti-arrestin3 siRNA was determined using the GeneGnome image analysis system and software (Syngene, Cambridge, UK). Absorbance values were normalized to those obtained after transfection with negative-control siRNA. Data are expressed as means ± SEM from four separate experiments, from four separate patient donors. **$P < 0.01$, significantly different from arrestin expression in negative-control transfected or non-transfected cells (one-way ANOVA; Dunnett's *post hoc* test).

receptor activity. Usually GPCR desensitization experiments compare responses generated in the presence or absence of agonist pre-treatment (Willets *et al.*, 2008). However, because CB receptor ligands are highly hydrophobic and difficult to wash out of experimental tissues, we established an alternative desensitization protocol. Here, cells were exposed to AEA (10 μM) for varying pre-incubation time periods before addition of the AC activator, forskolin (10 μM, for 10 min). Initial studies indicated that the ability of AEA to activate CB_1 receptor-mediated inhibition of AC diminished with increasing periods of AEA pre-incubation, and the observed time-course of CB_1 receptor inactivation, was similar to that reported previously when CB_1 receptors were exogenously expressed in HEK293 cells (Wu *et al.*, 2008). Analysis of the temporal profiles of AEA/ CB_1 receptor-activated AC inhibition and pERK1/2 signals shows that the ability of AEA to inhibit AC signalling declined more rapidly than its ability to signal through ERK1/2, although by 60 min AEA was unable to activate either signal. Collectively, these data highlight a sequential inhibition of CB_1 receptor signalling pathways.

An inherent problem with many biologically active molecules including endocannabinoids is that they are subject to enzymatic (FAAH) and other forms of degradation, possibly explaining why CB_1 receptor responsiveness declined over the experimental period. To address this possibility we applied our UPLC-ESI-MS/MS technique to measure free AEA concentrations in the assay buffer. Surprisingly, initial data showed that although 10 μM AEA was applied to the cell buffer, even with no pre-incubation period and regardless of the presence of cells, the free AEA concentration was actually 75% lower (2.5 μM). The highly lipophilic properties of AEA (Oddi *et al.*, 2010) possibly explain why free AEA concentrations are considerably lower than that originally applied, as this endocannabinoid is liable to stick to cell culture plasticware (Oddi *et al.*, 2010), and is also likely to be absorbed into cell membranes and/or bound to cell proteins (Makriyannis *et al.*, 2005). However, the continued decline of AEA concentrations in the presence of cells over the time-course of the experiment to a steady concentration of ~500 nM was prevented following FAAH or COX inhibition, suggesting that both enzymes contribute to AEA depletion. As AEA requires internalization before enzymatic degradation, the uptake process is liable to play a significant role in the depletion of extracellular AEA (Oddi *et al.*, 2010). It is nevertheless interesting to note that the temporal profiles of CB_1 receptor responsiveness to AEA were identical in the presence of the metabolically stable AEA-derivative methanandamide, or following FAAH inhibition. AEA can also be metabolized by

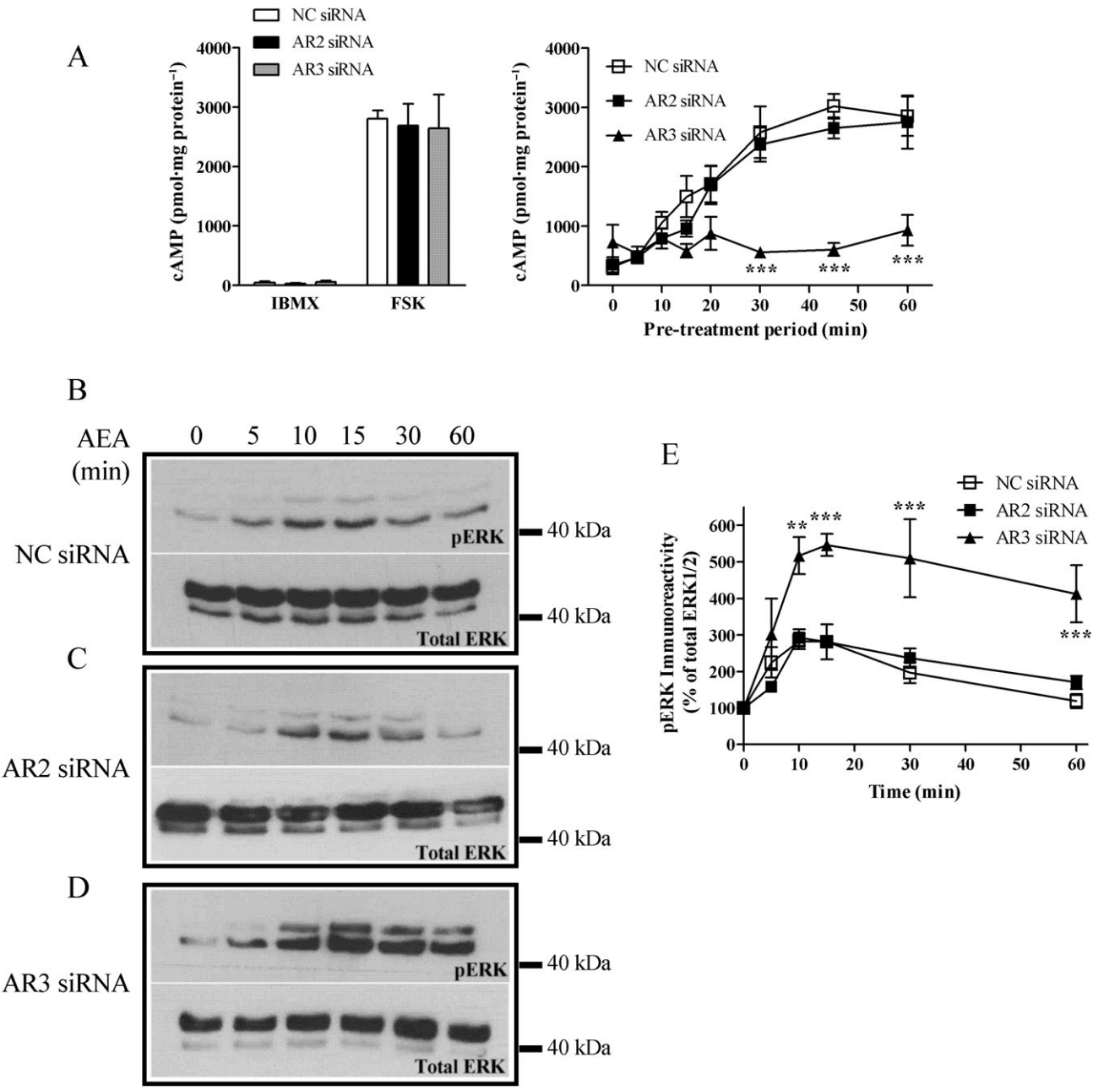

Figure 9

Arrestin3 suppression prevents CB_1 receptor desensitization and enhances AEA-stimulated ERK signalling. Arrestin2 and 3 expression was depleted after transfection of anti-arrestin2 and anti-arrestin3 siRNAs using the nucleofection techniques (A) After 48 h cells were exposed to a maximal concentration of AEA (10 μM) for varying periods before addition of the AC activator forskolin (Fsk; 10 μM) for a further 10 min to assess the effects of arrestin knockdown on CB_1 receptor desensitization. After forskolin addition, cAMP accumulation was terminated with ice-cold trichloroacetic acid, before cellular cAMP was extracted, and levels determined by radioreceptor assay. Data are shown as means ± SEM for six cell preparation from six separate patient donors. ***$P < 0.001$, significant inhibition of forskolin-stimulated cAMP production in the presence of arrestin3 siRNA (one-way ANOVA; Dunnett's *post hoc* test, compared with arrestin2 or negative-control treated cells). For ERK assays, cells were serum-starved for the final 24 h before incubation with AEA (10 μM) for various times. Cells were then lysed and pERK1/2 levels determined by immunoblotting techniques. Representative Western blots (upper panels) show the time-course of AEA-stimulated ERK1 (44 kDa)/2 (42 kDa) phosphorylation in the cells transfected with (B) negative-control (NC, 50 nM), (C) anti-arrestin2 (AR2, 50 nM) or (D) anti-arrestin3 (10 nM) siRNAs. To verify equal gel loading all blots were stripped and reprobed with anti-ERK1 antibody (lower panels). (E) Cumulative densitometric analysis shows that AEA-stimulated ERK1/2 phosphorylation is significantly enhanced and prolonged in the presence of arrestin3 siRNA (**$P < 0.01$, ***$P < 0.001$, significantly different from negative-control or arrestin2 siRNA treated cells (two-way ANOVA; Bonferroni's *post hoc* test). Data are means ± SEM from four separate experiments, from four separate patient donors.

many other enzymes including COXs, potentially producing a plethora of other bioactive compounds with diverse bioactivities (Vandevoorde and Lambert, 2007). Here, we show that the profile of AEA-mediated AC inhibition and ERK1/2 signalling through the CB_1 receptor was unaffected following COX inhibition. When combined with the finding that inhibition of AEA metabolism had no effect upon the magnitude of AEA/ CB_1 receptor-driven AC inhibition or ERK phosphorylation, it appears that our data strongly suggest that the loss of CB_1 receptor responsiveness occurred as a consequence of receptor desensitization, rather than depletion of available agonist.

Arrestin proteins have well-documented roles as negative regulators of GPCR signalling (DeWire *et al.*, 2007) and are recruited to agonist-occupied GPCRs after phosphorylation by GPCR kinases (GRK) (Willets *et al.*, 2003). The arrestins sterically inhibit GPCR/G-protein interactions, promoting desensitization and receptor internalization (Willets *et al.*, 2003; DeWire *et al.*, 2007). CB_1 receptors are substrates for GRK (Jin *et al.*, 1999), and removal of two putative GRK phosphorylation sites (T461A/S466A) in the C-terminal tail of CB_1 receptors prevented arrestin3 recruitment in HEK293 cells (Daigle *et al.*, 2008), which infers that arrestin proteins may well play a role in regulating CB_1 receptor signalling. Here using specific siRNA techniques to deplete individual arrestin expression, we show for the first time that the presence of arrestin3 is essential for AEA-stimulated CB_1 receptor desensitization in primary human myometrial cells. It is also interesting to note that following suppression of arrestin3 expression, that even relatively low (nM) concentrations of AEA were still capable of maximally activating CB_1 receptor-mediated AC inhibition even after 1 h agonist pre-incubation, which further emphasizes that the loss of CB_1 receptor responsiveness was due to desensitization and not agonist depletion. Collectively, our data also highlight that the potency of AEA to activate CB_1 receptor signalling has been greatly underestimated in previous studies.

Aside from their established roles promoting receptor desensitization and internalization (DeWire *et al.*, 2007) for an increasing number of GPCRs, arrestin proteins are reported to act as agonist-adaptor scaffolds to regulate MAPK signalling, enabling the GPCR/arrestin complex to undertake a diverse array of alternate signalling functions within the cell (DeWire *et al.*, 2007). Focus has been directed mainly on the ability of arrestins to scaffold ERK1/2 to the GPCR, leading to retention of active ERK1/2 within the cytoplasm and prolongation of signalling (DeWire *et al.*, 2007). Consistent with this previously reported role, one would predict that knockdown of arrestin3 would result in a dramatic attenuation of AEA/ CB_1 receptor-stimulated pERK1/2 signals, particularly during the sustained activation phase. Contrastingly, in primary myometrial cells arrestin3 knockdown strikingly enhanced CB_1 receptor-stimulated pERK1/2 signals. Our findings are similar to those reported in mouse embryonic fibroblast cells, whereby the magnitude and duration of α_{2A}-adrenoreceptor-mediated ERK signalling was markedly enhanced in the absence of arrestins2 and 3 (Wang *et al.*, 2006b). Endogenous α_{2A}-adrenoreceptors evoke ERK1/2 phosphorylation equally efficiently through Src-dependent and Src-independent pathways, which subsequently converge on the Ras-Raf-MEK pathway (Wang *et al.*, 2006b). Interestingly, the Src-dependent pathway requires arrestin proteins to recruit Src to the signalling complex and, in the absence of arrestin, the Src-independent pathway becomes dominant, resulting in enhanced ERK1/2 signals and more rapid translocation of the signalling complex to the nucleus (Wang *et al.*, 2006b). As Src and arrestin3 both play a role in regulating CB_1 receptor-mediated ERK1/2 phosphorylation, it is possible that arrestin3 undertakes a similar role in the regulation of AEA/ CB_1 receptor-mediated ERK1/2 signalling in myometrial cells. Furthermore, our data suggest that arrestin3 might be the key arrestin isoform mediating the equivalent task for the α_{2A}-adrenoreceptor (Wang *et al.*, 2006b).

In summary, we report the presence of many of the components of the endocannabinoid system in primary myometrial cells, including the presence of functional CB_1 receptors. Moreover we have characterized several AEA/ CB_1 receptor-stimulated signalling pathways, identifying arrestin3 as a key negative regulator of CB_1 receptor responsiveness and ERK1/2 signalling. At present the physiological relevance of CB_1 receptor signalling in the myometrium is largely unknown. However, the fact that marijuana use is associated with preterm labour combined with our findings that serum AEA concentrations are elevated during active labour suggests a role for CB_1 receptor signalling in labour. Indeed, raised AEA concentrations imply enhanced signalling through CB_1 receptor pathways such as ERK1/2, which considering the previously reported role that myometrial COX2 expression is enhanced through ERK1/2 signalling (Molnar *et al.*, 1999), potentially highlights a role for AEA/ CB_1 receptor regulation of prostaglandin production and induction of labour. As AEA/ CB_1 receptor/ERK1/2 signalling is negatively regulated by arrestin3, the expression of this protein during labour may also play an important role in regulating prostaglandin production. However, despite evidence that GRK isoenzyme levels are differentially expressed through pregnancy (Brenninkmeijer *et al.*, 1999), levels of arrestin isoform expression remain to be investigated.

Acknowledgement

We thank Robert J. Lefkowitz (Duke University, USA) for kindly providing the arrestin (A1CT) antibody.

Conflict of interest

None.

References

Abadji V, Lin S, Taha G, Griffin G, Stevenson LA, Pertwee RG *et al.* (1994). (R)-methanandamide: a chiral novel anandamide possessing higher potency and metabolic stability. J Med Chem 37: 1889–1893.

Ahn S, Nelson CD, Garrison TR, Miller WE, Lefkowitz RJ (2003). Desensitization, internalization, and signaling functions of β-arrestins demonstrated by RNA interference. Proc Natl Acad Sci USA 100: 1740–1744.

Alexander SPH, Mathie A, Peters JA (2009). Guide to Receptors and Channels (GRAC), 4th edn. Br J Pharmacol 158 (Suppl. 1): S1–S254.

Bambang KN, Karasu T, Gebeh A, Taylor AH, Marczylo TH, Lam P *et al.* (2010). From fertilization to implantation in mammalian pregnancy-modulation of early human reproduction by the endocannabinoid system. Pharmaceuticals 3: 2910–2929.

Bisogno T, Melck D, Bobrov M, Gretskaya NM, Bezuglov VV, De Petrocellis L *et al.* (2000). N-acyl-dopamines: novel synthetic CB_1 cannabinoid-receptor ligands and inhibitors of anandamide inactivation with cannabimimetic activity in vitro and in vivo. Biochem J 351: 817–824.

Brenninkmeijer CB, Price SA, Lopez Bernal A, Phaneuf S (1999). Expression of G-protein-coupled receptor kinases in pregnant term and non-pregnant human myometrium. J Endocrinol 162: 401–408.

Brighton PJ, McDonald J, Taylor AH, Challiss RA, Lambert DG, Konje JC *et al.* (2009). Characterization of anandamide-stimulated cannabinoid receptor signaling in human ULTR myometrial smooth muscle cells. Mol Endocrinol 23: 1415–1427.

Brown BL, Albano JD, Ekins RP, Sgherzi AM (1971). A simple and sensitive saturation assay method for the measurement of adenosine 3′:5′-cyclic monophosphate. Biochem J 121: 561–562.

Cheng Y, Prusoff WH (1973). Relationship between the inhibition constant (K_1) and the concentration of inhibitor which causes 50 per cent inhibition (I_{50}) of an enzymatic reaction. Biochem Pharmacol 22: 3099–3108.

Chomczynski P, Mackey K (1995). Substitution of chloroform by bromo-chloropropane in the single-step method of RNA isolation. Anal Biochem 225: 163–164.

Daigle TL, Kwok ML, Mackie K (2008). Regulation of CB1 cannabinoid receptor internalization by a promiscuous phosphorylation-dependent mechanism. J Neurochem 106: 70–82.

Dennedy MC, Friel AM, Houlihan DD, Broderick VM, Smith T, Morrison JJ (2004). Cannabinoids and the human uterus during pregnancy. Am J Obstet Gynecol 190: 2–9; discussion 3A.

DeWire SM, Ahn S, Lefkowitz RJ, Shenoy SK (2007). β-arrestins and cell signaling. Annu Rev Physiol 69: 483–510.

El-Talatini MR, Taylor AH, Konje JC (2009a). Fluctuation in anandamide levels from ovulation to early pregnancy in in-vitro fertilization-embryo transfer women, and its hormonal regulation. Hum Reprod 24: 1989–1998.

El-Talatini MR, Taylor AH, Konje JC (2009b). The relationship between plasma levels of the endocannabinoid, anandamide, sex steroids, and gonadotrophins during the menstrual cycle. Fertil Steril 93: 1986–1996.

Grimsey NL, Goodfellow CE, Scotter EL, Dowie MJ, Glass M, Graham ES (2008). Specific detection of CB1 receptors; cannabinoid CB1 receptor antibodies are not all created equal! J Neurosci Methods 171: 78–86.

Habayeb OM, Taylor AH, Evans MD, Cooke MS, Taylor DJ, Bell SC *et al.* (2004). Plasma levels of the endocannabinoid anandamide in women – a potential role in pregnancy maintenance and labor? J Clin Endocrinol Metab 89: 5482–5487.

Habayeb OM, Taylor AH, Finney M, Evans MD, Konje JC (2008). Plasma anandamide concentration and pregnancy outcome in women with threatened miscarriage. JAMA 299: 1135–1136.

Jin W, Brown S, Roche JP, Hsieh C, Celver JP, Kovoor A *et al.* (1999). Distinct domains of the CB1 cannabinoid receptor mediate desensitization and internalization. J Neurosci 19: 3773–3780.

Kawahara H, Drew GM, Christie MJ, Vaughan CW (2010). Inhibition of fatty acid amide hydrolase unmasks CB_1 receptor and TRPV1 channel-mediated modulation of glutamatergic synaptic transmission in midbrain periaqueductal grey. Br J Pharmacol 163: 1214–1222.

Lam PM, Marczylo TH, El-Talatini M, Finney M, Nallendran V, Taylor AH *et al.* (2008). Ultra performance liquid chromatography tandem mass spectrometry method for the measurement of anandamide in human plasma. Anal Biochem 380: 195–201.

Lowry OH, Rosebrough NJ, Farr AL, Randall RJ (1951). Protein measurement with the Folin phenol reagent. J Biol Chem 193: 265–275.

Maccarrone M (2009). Endocannabinoids: friends and foes of reproduction. Prog Lipid Res 48: 344–354.

Maccarrone M, Valensise H, Bari M, Lazzarin N, Romanini C, Finazzi-Agro A (2000). Relation between decreased anandamide hydrolase concentrations in human lymphocytes and miscarriage. Lancet 355: 1326–1329.

Makriyannis A, Tian X, Guo J (2005). How lipophilic cannabinergic ligands reach their receptor sites. Prostaglandins Other Lipid Mediat 77: 210–218.

Molnar M, Rigo J Jr, Romero R, Hertelendy F (1999). Oxytocin activates mitogen-activated protein kinase and up-regulates cyclooxygenase-2 and prostaglandin production in human myometrial cells. Am J Obstet Gynecol 181: 42–49.

O'Sullivan SE (2007). Cannabinoids go nuclear: evidence for activation of peroxisome proliferator-activated receptors. Br J Pharmacol 152: 576–582.

Oddi S, Fezza F, Catanzaro G, De Simone C, Pucci M, Piomelli D *et al.* (2010). Pitfalls and solutions in assaying anandamide transport in cells. J Lipid Res 51: 2435–2444.

Paria BC, Das SK, Dey SK (1995). The preimplantation mouse embryo is a target for cannabinoid ligand-receptor signaling. Proc Natl Acad Sci USA 92: 9460–9464.

Park B, Gibbons HM, Mitchell MD, Glass M (2003). Identification of the CB1 cannabinoid receptor and fatty acid amide hydrolase (FAAH) in the human placenta. Placenta 24: 990–995.

Ross RA, Brockie HC, Stevenson LA, Murphy VL, Templeton F, Makriyannis A *et al.* (1999). Agonist-inverse agonist characterization at CB1 and CB2 cannabinoid receptors of L759633, L759656, and AM630. Br J Pharmacol 126: 665–672.

Sale S, Fong IL, de Giovanni C, Landuzzi L, Brown K, Steward WP *et al.* (2009). APC10.1 cells as a model for assessing the efficacy of potential chemopreventive agents in the Apc(Min) mouse model in vivo. Eur J Cancer 45: 2731–2735.

Taylor AH, Ang C, Bell SC, Konje JC (2007). The role of the endocannabinoid system in gametogenesis, implantation and early pregnancy. Hum Reprod Update 13: 501–513.

Taylor AH, Amoako AA, Bambang K, Karasu T, Gebeh A, Lam PM *et al.* (2010). Endocannabinoids and pregnancy. Clin Chim Acta 411: 921–930.

Trabucco E, Acone G, Marenna A, Pierantoni R, Cacciola G, Chioccarelli T *et al.* (2009). Endocannabinoid system in first trimester placenta: low FAAH and high CB1 expression characterize spontaneous miscarriage. Placenta 30: 516–522.

Vandevoorde S, Lambert DM (2007). The multiple pathways of endocannabinoid metabolism: a zoom out. Chem Biodivers 4: 1858–1881.

Wang H, Xie H, Dey SK (2006a). Endocannabinoid signaling directs periimplantation events. AAPS J 8: E425–E432.

Wang Q, Lu R, Zhao J, Limbird LE (2006b). Arrestin serves as a molecular switch, linking endogenous alpha2-adrenergic receptor to SRC-dependent, but not SRC-independent, ERK activation. J Biol Chem 281: 25948–25955.

Wenger T, Fragkakis G, Giannikou P, Probonas K, Yiannikakis N (1997). Effects of anandamide on gestation in pregnant rats. Life Sci 60: 2361–2371.

Willets J, Kelly E (2001). Desensitization of endogenously expressed δ-opioid receptors: no evidence for involvement of G protein-coupled receptor kinase 2. Eur J Pharmacol 431: 133–141.

Willets JM, Challiss RA, Nahorski SR (2003). Non-visual GRKs: are we seeing the whole picture? Trends Pharmacol Sci 24: 626–633.

Willets JM, Taylor AH, Shaw H, Konje JC, Challiss RA (2008). Selective regulation of H_1 histamine receptor signaling by G protein-coupled receptor kinase 2 in uterine smooth muscle cells. Mol Endocrinol 22: 1893–1907.

Wu DF, Yang LQ, Goschke A, Stumm R, Brandenburg LO, Liang YJ *et al*. (2008). Role of receptor internalization in the agonist-induced desensitization of cannabinoid type 1 receptors. J Neurochem 104: 1132–1143.